


 Cite this: *RSC Adv.*, 2016, 6, 64871

Highly improved dielectric properties of polymer/ α -Fe₂O₃ composites at elevated temperatures

Kenichi Hayashida

α -Fe₂O₃ particles were incorporated into ten kinds of polymer matrices, and the dielectric properties of the resultant polymer/ α -Fe₂O₃ composites were investigated between 40 °C and 160 °C. We found that the dielectric properties strongly depended not only on the temperatures but also on the kind of polymer matrices. For engineering plastics such as polyetherimide (PEI), the dielectric constant ϵ'_r was highly enhanced at around 1 kHz by incorporation of the α -Fe₂O₃ particles owing to Maxwell–Wagner polarization of free electrons in the α -Fe₂O₃ particles. This is probably because the π electrons in the aromatic structures of the engineering plastics strongly interact with the electrons in the α -Fe₂O₃ particles. Furthermore, the dielectric loss factor ϵ''_r for the engineering plastics became small at elevated temperatures because the conductivity of the α -Fe₂O₃ particle was enhanced and therefore the relaxation frequency of Maxwell–Wagner polarization was shifted to higher frequency. PEI/ α -Fe₂O₃ composites exhibited highly improved dielectric properties at around 1 kHz, the high ϵ'_r and very low ϵ''_r at the elevated temperatures above 120 °C. It was demonstrated that the PEI/ α -Fe₂O₃ composite was comparable to the PEI/BaTiO₃ composite in dielectric performance at 160 °C. Because the cost of α -Fe₂O₃ is much lower than that of BaTiO₃, the PEI/ α -Fe₂O₃ composite might be promising as a low-cost dielectric material for high-temperature applications.

Received 16th May 2016

Accepted 3rd July 2016

DOI: 10.1039/c6ra12752e

www.rsc.org/advances

Introduction

Dielectric materials are mainly used in capacitors to store electrical energy.^{1–3} In comparison to ceramic materials, polymer ones have the advantages of low cost, lightweight and high processability. However, the very low dielectric constant ϵ'_r of the polymer material strongly prevents improvement of the capacitors. Therefore, polymer/ceramic composite materials have been much studied over the last few decades. Among the ceramics, BaTiO₃ has been most widely used for enhancement in the ϵ'_r of polymer materials because of the very high ϵ'_r of BaTiO₃.^{4–21} However, the high cost of BaTiO₃ is a serious problem for industrial applications.

On the other hand, hematite (α -Fe₂O₃) is a very low cost ceramic material although α -Fe₂O₃ has not been paid attention as a high ϵ'_r filler for polymer materials owing to the low ϵ'_r of α -Fe₂O₃; according to the reported literature, the ϵ'_r of α -Fe₂O₃ is as low as 30.^{22–27} Therefore, few studies are available on the dielectric properties of polymer/ α -Fe₂O₃ composites.^{28–30} Djoković and coworkers reported dielectric properties of a composites epoxy resin and α -Fe₂O₃ nanorods.²⁸ Also, α -Fe₂O₃ nanorods were dispersed in a poly(vinyl alcohol)/poly(ethylene glycol) blend by Sayed *et al.*²⁹ There are only small improvements of the ϵ'_r s of the polymer materials in these studies.

In this paper, we focus on the conductivity σ of α -Fe₂O₃ at elevated temperatures. Typically, α -Fe₂O₃ is known to have σ of about 10^{−5} to 10^{−6} S cm^{−1} at room temperature.²⁶ The σ of semiconductors such as α -Fe₂O₃ is enhanced as temperature is raised because electrons are excited from a valence band to a conductive band.³¹ It is expected that the σ of α -Fe₂O₃ is especially increased owing to its narrow band gap of 2.1 eV.³² At elevated temperatures, the enhanced σ of the α -Fe₂O₃ particles would bring a high ϵ'_r to a polymer/ α -Fe₂O₃ composite owing to Maxwell–Wagner polarization³³ of the resultant free electrons in the α -Fe₂O₃ particles. The polymer/ α -Fe₂O₃ composite might be promising as a low-cost dielectric material for high-temperature applications such as hybrid and electric vehicles.^{34,35} In this study, α -Fe₂O₃ particles were incorporated into ten kinds of polymer matrices, and the dielectric properties of the polymer/ α -Fe₂O₃ composites were investigated between 40 °C and 160 °C. We found that the dielectric properties strongly depended not only on the temperatures but also on the kind of polymer matrices. Furthermore, the dielectric performance of one of the polymer/ α -Fe₂O₃ composite was compared with that of a corresponding polymer/BaTiO₃ composite at the elevated temperatures.

Experimental

Sample preparation

α -Fe₂O₃ particles were obtained from Kanto Chemical (Japan). The density and specific area of the α -Fe₂O₃ particles were

Materials and Processing Dept. II, Toyota Central R&D Labs., Inc., Nagakute, Aichi 480-1192, Japan. E-mail: e1440@mosk.tytlabs.co.jp



determined to be 4.94 g cm^{-3} and $8.71 \text{ m}^2 \text{ g}^{-1}$ using helium pycnometry and a standard BET method, respectively. The average diameter of the $\alpha\text{-Fe}_2\text{O}_3$ particles was calculated to be 139 nm from the obtained density and specific area data. In the same manner, the density, specific area and average diameter of BaTiO_3 particles obtained from Wako Pure Chemical Industries (Japan) were determined to be 5.73 g cm^{-3} , $9.99 \text{ m}^2 \text{ g}^{-1}$ and 105 nm, respectively.

Polystyrene (PS) and poly(methyl methacrylate) (PMMA) were purchased from Wako Pure Chemical Industries (Japan). Poly(2-vinylpyridine) (P2VP) was obtained from Scientific Polymer Products. Styrene/acrylonitrile copolymer (SAN) with 30 wt% of acrylonitrile, polyphenylene ether (PPE), polysulfone (PSF), polyethersulfone (PES) and polyetherimide (PEI) were purchased from Sigma-Aldrich. Styrene/*N*-phenylmaleimide alternating copolymer (St-PMI)³⁶ and polyarylate (PAR)³⁷ were synthesized using reported methods, where PAR contained equimolar amounts of isophthaloyl and terephthaloyl moieties.

A series of polymer/ $\alpha\text{-Fe}_2\text{O}_3$ composites were prepared by simply blending the $\alpha\text{-Fe}_2\text{O}_3$ particles with the polymer matrices. First, the $\alpha\text{-Fe}_2\text{O}_3$ particles and the polymer matrix except PES were homogeneously dispersed in 1,4-dioxane by sonication. The dispersion was quickly frozen by liquid nitrogen, and then freeze-dried under vacuum. For preparation of PES/ $\alpha\text{-Fe}_2\text{O}_3$ composites, dichloromethane was used instead of 1,4-dioxane because PES was insoluble in 1,4-dioxane. Subsequently, all the pre-mixtures thus-obtained were further

kneaded in molten states. Also, PEI/ BaTiO_3 composites were prepared in the same manner. The resultant composites were hot-pressed into disklike specimens with a diameter of 33 mm and a thickness of ~ 0.52 mm. For electrical measurements, two gold electrodes with a diameter of 27 mm were deposited on the top and bottom of the specimens.

Measurements

Complex permittivity was obtained in the frequency f range of 10^2 to 10^6 Hz at 2 V using an LCR meter (E4980A, Agilent) coupled with a rheometer (ARES G2, TA instruments). The temperature of the specimen was controlled in the oven of the rheometer. Direct current (DC) resistance of the specimen was measured at room temperature under a nitrogen atmosphere using a megohmmeter (SM-8220, Hioki), and the value was recorded after 10 minute from application of a voltage of 500 V. The cross-section of the specimen that had been flattened with argon ion beam³⁸ was observed using an SEM (S-4300, Hitachi) operated at an accelerating voltage of 2 kV.

Results and discussion

Dielectric properties of polymer/ $\alpha\text{-Fe}_2\text{O}_3$ composites at 40 °C

We prepared a series of polymer/ $\alpha\text{-Fe}_2\text{O}_3$ composites with the volume fraction Φ of $\alpha\text{-Fe}_2\text{O}_3$, $\Phi = 0.2$. The chemical structures of the polymer matrices are shown in Fig. 1. All the polymers are

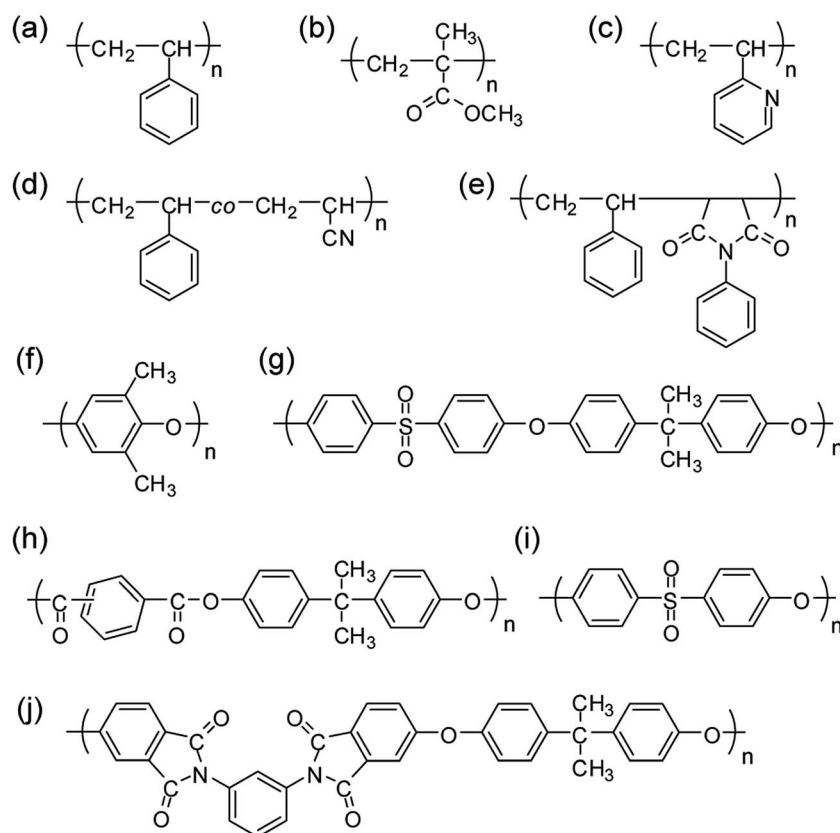


Fig. 1 Chemical structures of polymer matrices used in this study. (a) PS. (b) PMMA. (c) P2VP. (d) SAN. (e) St-PMI. (f) PPE. (g) PSF. (h) PAR. (i) PES. (j) PEI.



Table 1 Dielectric characteristics (1 kHz) for polymer/ α -Fe₂O₃ composites with $\Phi = 0.2$ obtained at 40 °C

Polymer	ϵ'_r	ϵ''_r	ϵ'_r polymer ^a	ϵ'_r Fe ₂ O ₃ ^b
PS	4.12	0.123	2.58	27.8
PMMA	5.25	0.453	3.39	31.2
P2VP	6.34	0.447	4.22	33.3
SAN	5.05	0.286	3.03	40.5
PSF	5.71	0.339	3.13	66.2
St-PMI	5.59	0.182	2.88	83.4
PAR	6.52	0.402	3.27	109
PEI	6.23	0.250	3.09	109
PES	7.13	0.475	3.52	116
PPE	5.58	0.162	2.63	120

^a ϵ'_r of the polymer matrix only. ^b Apparent ϵ'_r of α -Fe₂O₃ calculated using Lichteneker's logarithmic mixing rule.

popular, and some of them are engineering plastics that can be used over 150 °C (Fig. 1f–j). The ϵ'_r and dielectric loss factor ϵ''_r values of the polymer/ α -Fe₂O₃ composites (1 kHz, 40 °C) were listed in Table 1. There is a weak tendency for the ϵ'_r of the composites prepared using the engineering plastics to be high. This is an interesting phenomenon that has never been reported. However, it is difficult to correctly evaluate the ϵ'_r enhancement effect by direct comparing of the ϵ'_r values of the composites because each ϵ'_r of the polymer matrix ϵ'_r polymer is different to some extent as shown in Table 1. Therefore, we suggest that apparent ϵ'_r of α -Fe₂O₃, ϵ'_r Fe₂O₃ is calculated using Lichteneker's logarithmic mixing rule and then compared in order to separate a contribution of the ϵ'_r polymer itself from the ϵ'_r of the composite. It is known that the ϵ'_r of a polymer/filler composite often obeys Lichteneker's logarithmic mixing rule as follows:^{4,7,9,15–17,39}

$$\epsilon'_r = \epsilon'_r \text{ polymer} (\epsilon'_r \text{ filler} / \epsilon'_r \text{ polymer})^\Phi, \quad (1)$$

where ϵ'_r filler and Φ are the ϵ'_r and volume fraction of the filler. Notice that the ϵ'_r filler is not the ϵ'_r of the filler itself but an apparent ϵ'_r of the filler particles in the polymer matrix.

Generally, the ϵ'_r filler is much smaller than the ϵ'_r of the corresponding bulk compound, mainly because the filler particles do not form a continuous phase in the polymer/filler composite system; the ϵ'_r filler is significantly reduced by the interface between the filler particles. Furthermore, the ϵ'_r filler is affected not only by the size and form of the filler particle but also by the dispersivity of the filler particles in the matrix.¹⁶ For example, the apparent ϵ'_r of spherical BaTiO₃ nanoparticles with a diameter of less than 100 nm is reported to be around 100 according to literatures.^{8,39}

The calculated ϵ'_r Fe₂O₃ is shown in Table 1. There is a strong dependency of the ϵ'_r Fe₂O₃ on the polymer matrix; the ϵ'_r Fe₂O₃ is about 30 for PS, PMMA and P2VP whereas over 100 for PAR, PEI, PES and PPE. In other word, the ϵ'_r for engineering plastics is more enhanced by the α -Fe₂O₃ particles than that for general-purpose plastics such as PS and PMMA. Fig. 2 shows the frequency f dependences of the ϵ'_r and ϵ''_r of four kinds of composites for PEI, PSF, PPE and PS with $\Phi = 0.2$ obtained at 40 °C. Every ϵ'_r is decreased as f is increased. This is because the dielectric relaxation of a polarization occurs in the f range, which results in a ϵ''_r peak as shown in Fig. 2b. This polarization would be attributed to the interfacial polarization of free electrons in the α -Fe₂O₃ particles, that is Maxwell–Wagner polarization.³³ Because the relaxation frequency becomes high as the σ of the α -Fe₂O₃ particles is high for Maxwell–Wagner polarization, it is suggested that the σ of the α -Fe₂O₃ particles in the PEI/ α -Fe₂O₃ and PPE/ α -Fe₂O₃ composites is higher than that in the PS/ α -Fe₂O₃ composite, resulting in the higher ϵ'_r Fe₂O₃ for PEI and PPE over the reported value of ~ 30 .^{22–27} This is probably because the π electrons in the aromatic structures of the engineering plastics strongly interact with the electrons in the α -Fe₂O₃ particles. Also, it is suggested that the enhanced ϵ'_r Fe₂O₃ is caused by the dispersivity of the α -Fe₂O₃ particles in the polymer matrix and the interfacial state between the α -Fe₂O₃ particles and the polymer matrix. However, it is difficult to explain the strong frequency dependence of the dielectric properties as shown in Fig. 2 by these two contributions (the dispersivity and the interfacial state). Therefore, we conclude

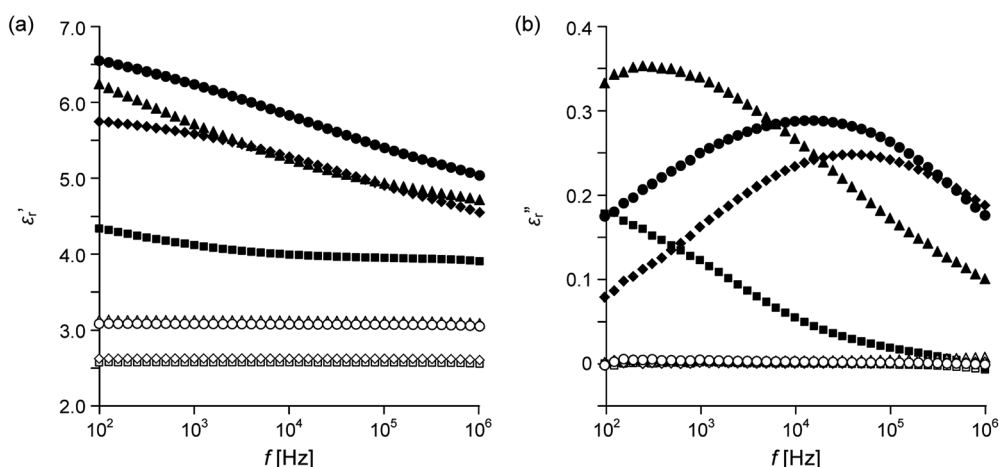


Fig. 2 Frequency f dependence of (a) ϵ'_r and (b) ϵ''_r of polymer/ α -Fe₂O₃ composites with $\Phi = 0$ (open symbols) and $\Phi = 0.2$ (filled symbols) obtained at 40 °C. The polymer matrices are PEI (circles), PSF (triangles), PPE (diamonds) and PS (squares).



that the enhanced $\epsilon'_{r \text{ Fe}_2\text{O}_3}$ is mainly due to the interaction between the electrons in the $\alpha\text{-Fe}_2\text{O}_3$ particles and the polymer matrix. From the viewpoint of the molecular structures of the polymer matrix, the $\alpha\text{-Fe}_2\text{O}_3$ particles might be more effective for fully aromatic polyester and polyimide with long conjugations.

Dielectric properties of polymer/ $\alpha\text{-Fe}_2\text{O}_3$ composites at 160 °C

The PEI/ $\alpha\text{-Fe}_2\text{O}_3$ and PPE/ $\alpha\text{-Fe}_2\text{O}_3$ composites are not useful at 40 °C owing to the large ϵ''_r values over 0.1 (Table 1). Under an electric field E , the power loss of a dielectric material per unit volume, P is expressed as,¹⁶

$$P = E^2 \times 2\pi f \epsilon_0 \epsilon''_r, \quad (2)$$

where ϵ_0 is the permittivity of vacuum. Because P is proportional to ϵ''_r , the ϵ''_r of the material must be low for industrial applications such as capacitors.

The large ϵ''_r values of the polymer/ $\alpha\text{-Fe}_2\text{O}_3$ composites are drastically reduced at 160 °C. Dielectric characteristics (1 kHz) obtained at 160 °C were listed in Table 2 for six kinds of polymer/ $\alpha\text{-Fe}_2\text{O}_3$ composites with $\Phi = 0.2$. At 1 kHz, all the ϵ''_r values are less than 0.05. Furthermore, for PEI, PSF, PAR and PES, the $\epsilon'_{r \text{ Fe}_2\text{O}_3}$ is more than 150 at 160 °C. For the four kinds of composites, the f dependences of the ϵ'_r and ϵ''_r are shown

Table 2 Dielectric characteristics (1 kHz) for polymer/ $\alpha\text{-Fe}_2\text{O}_3$ composites with $\Phi = 0.2$ obtained at 160 °C

Polymer	ϵ'_r	ϵ''_r	$\epsilon'_{r \text{ polymer}}^a$	$\epsilon'_{r \text{ Fe}_2\text{O}_3}^b$
St-PMI	5.95	0.0307	2.87	116
PPE	5.71	0.0110	2.61	139
PEI	6.73	0.0321	3.11	157
PSF	6.82	0.0525	3.12	165
PAR	7.29	0.0509	3.31	182
PES	8.32	0.0533	3.53	246

^a ϵ'_r of the polymer matrix only. ^b Apparent ϵ'_r of $\alpha\text{-Fe}_2\text{O}_3$ calculated using Lichtenecker's logarithmic mixing rule.

in Fig. 3. Because the dielectric relaxations of Maxwell–Wagner polarization are not started at around 1 kHz as shown in Fig. 3b, the ϵ''_r values are small in the lower f ranges than 1 kHz. This result indicates the σ of the $\alpha\text{-Fe}_2\text{O}_3$ particle is higher at 160 °C than 40 °C. Fig. 4 shows a variation in the f dependences of the ϵ'_r and ϵ''_r of the PEI/ $\alpha\text{-Fe}_2\text{O}_3$ composites with $\Phi = 0.2$ between 40 and 160 °C. The ϵ''_r peak is shifted to the higher f until the temperature reaches 120 °C.

For the four polymer matrices, we also prepared polymer/ $\alpha\text{-Fe}_2\text{O}_3$ composites with $\Phi = 0.4$. Fig. 5 shows the f dependences of the ϵ'_r and ϵ''_r of polymer/ $\alpha\text{-Fe}_2\text{O}_3$ composites with $\Phi = 0.4$ at 160 °C. The ϵ''_r of the PEI/ $\alpha\text{-Fe}_2\text{O}_3$ composite remains small whereas for PAR and PES, the ϵ''_r becomes very large over all the f range. In order to elucidate the large ϵ''_r , the volume resistivity ρ_{DC} of the composites was measured. At $\Phi = 0.4$, the ρ_{DC} for PAR and PES is much lower than that for PEI and PSF as shown in Fig. 6. ϵ''_r is the sum of a loss from σ , $\epsilon''_{r(\sigma)}$ and losses from dielectric polarizations $\epsilon''_{r(\text{DP})}$:⁴⁰

$$\epsilon''_r = \epsilon''_{r(\sigma)} + \epsilon''_{r(\text{DP})}. \quad (3)$$

Furthermore, $\epsilon''_{r(\sigma)}$ is described using ρ_{DC} as follows:

$$\epsilon''_{r(\sigma)} = 1/(2\pi f \epsilon_0 \rho_{\text{DC}}). \quad (4)$$

It is suggested that because $\epsilon''_{r(\sigma)}$ is inversely proportion to f and ρ_{DC} , the ϵ''_r is highly increased at the low f range for PAR and PES. The low ρ_{DC} for PAR and PES could be attributed to a leak current passing through the conductive networks of the $\alpha\text{-Fe}_2\text{O}_3$ particles, that is, percolation of the $\alpha\text{-Fe}_2\text{O}_3$ particles. According to the percolation theory with a random packing of spherical particles, the percolation threshold is calculated to be about 0.30.^{41,42} Therefore, it was reasonable that the percolation of the $\alpha\text{-Fe}_2\text{O}_3$ particles occurred in the polymer/ $\alpha\text{-Fe}_2\text{O}_3$ composites with $\Phi = 0.4$. To the contrary, it was unusual that the PEI/ $\alpha\text{-Fe}_2\text{O}_3$ composite had a high ρ_{DC} even at $\Phi = 0.4$. We suspected that the dispersivity of the $\alpha\text{-Fe}_2\text{O}_3$ particles in the polymer matrix was different between

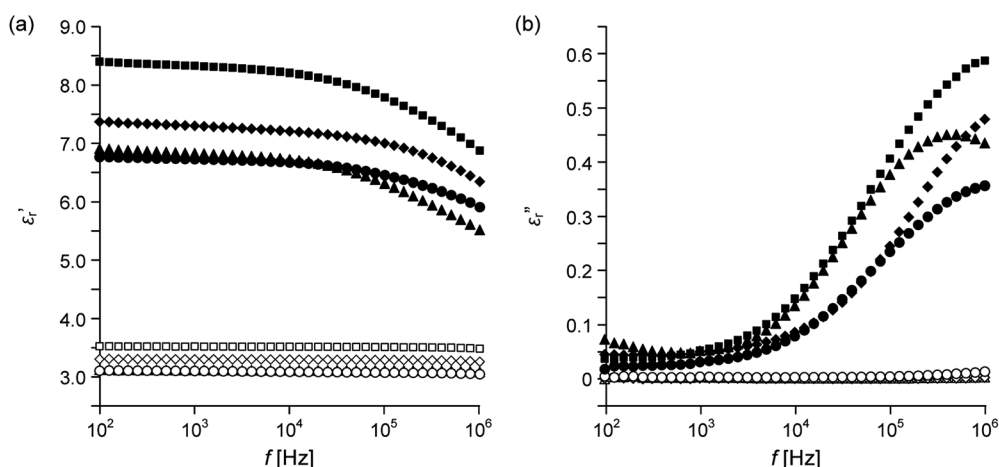


Fig. 3 Frequency f dependence of (a) ϵ'_r and (b) ϵ''_r of polymer/ $\alpha\text{-Fe}_2\text{O}_3$ composites with $\Phi = 0$ (open symbols) and $\Phi = 0.2$ (filled symbols) obtained at 160 °C. The polymer matrices are PEI (circles), PSF (triangles), PAR (diamonds) and PES (squares).



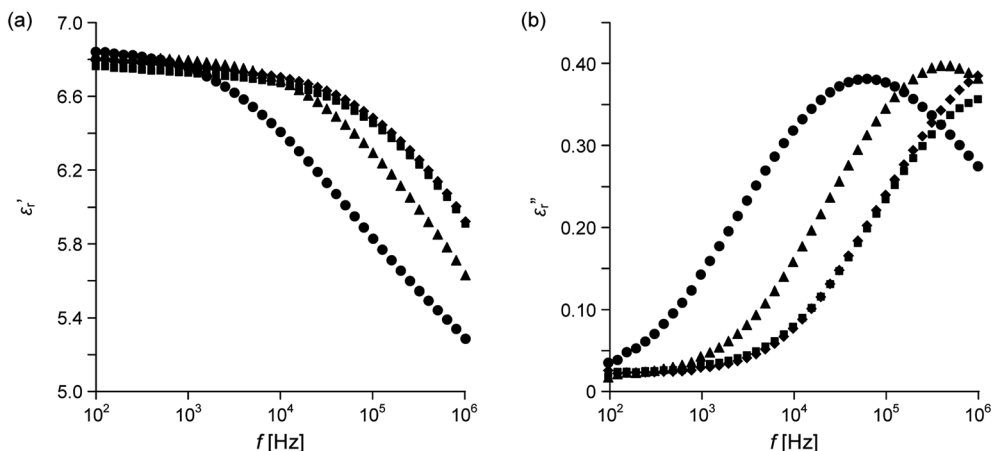


Fig. 4 Frequency f dependence of (a) ϵ'_r and (b) ϵ''_r of a PEI/ α -Fe₂O₃ composite with $\Phi = 0.2$ obtained at 40 °C (circles), 80 °C (triangles), 120 °C (diamonds) and 160 °C (squares).

the PEI/ α -Fe₂O₃ and PAR/ α -Fe₂O₃ composites, and observed it using SEM. Fig. 7 shows SEM images of the PEI/ α -Fe₂O₃ and PAR/ α -Fe₂O₃ composites with $\Phi = 0.20$ and $\Phi = 0.4$. There is no great difference in the dispersivity of the α -Fe₂O₃ particles, which means that the significant difference in ρ_{DC} is not due to the dispersivity of the α -Fe₂O₃ particles. In the PEI/ α -Fe₂O₃ composite, the α -Fe₂O₃ particles would be covered with a PEI layer at a nanometer scale, resulting in the high ρ_{DC} for PEI owing to inhibition of the tunneling conduction of the free electron^{39,43} between the α -Fe₂O₃ particles.

Comparing of dielectric performance for PEI/ α -Fe₂O₃ and PEI/BaTiO₃ composites

As mentioned above, the PEI/ α -Fe₂O₃ composite exhibits the high ϵ'_r and very low ϵ''_r at the elevated temperature above 120 °C, which might be promising as a low-cost dielectric material for high-temperature applications; PEI has a maximum operating temperature of 200 °C.³⁵ Therefore, the novel PEI/ α -Fe₂O₃ composite was compared with a conventional PEI/BaTiO₃

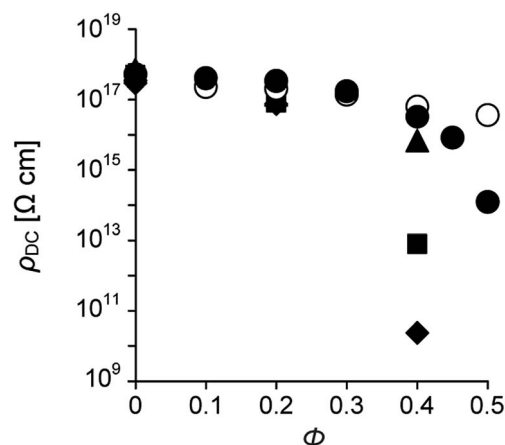


Fig. 6 Volume resistivity ρ_{DC} of polymer/ α -Fe₂O₃ (filled symbols) and PEI/BaTiO₃ (open symbols) composites as a function of Φ . The polymer matrices are PEI (circles), PSF (triangles), PAR (diamonds) and PES (squares).

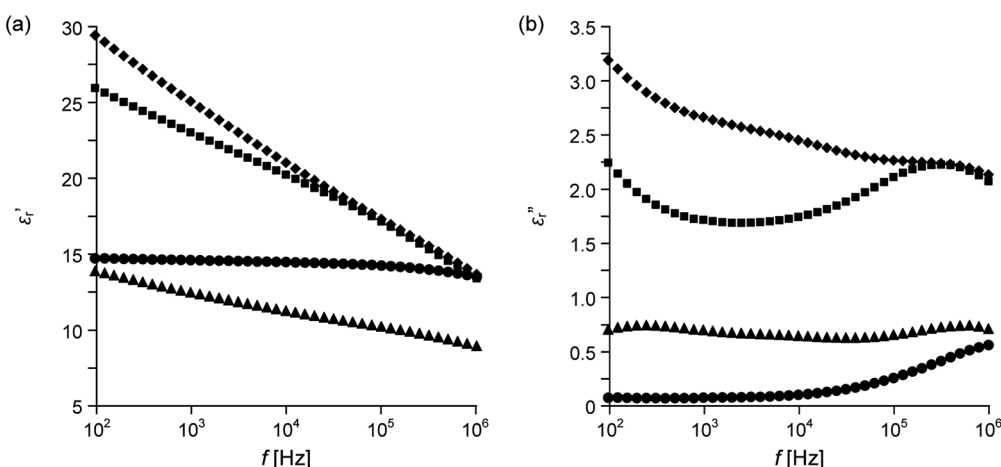


Fig. 5 Frequency f dependence of (a) ϵ'_r and (b) ϵ''_r of polymer/ α -Fe₂O₃ composites with $\Phi = 0.4$ obtained at 160 °C. The polymer matrices are PEI (circles), PSF (triangles), PAR (diamonds) and PES (squares).



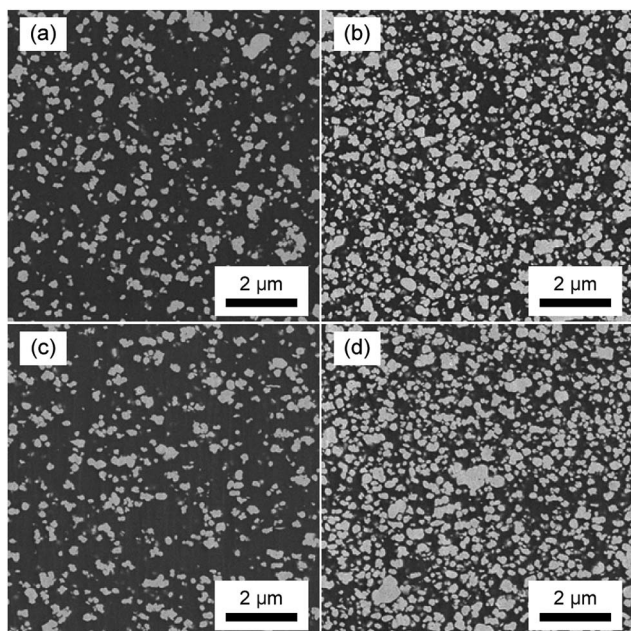


Fig. 7 SEM images of (a and b) PEI/ α -Fe₂O₃ and (c and d) PAR/ α -Fe₂O₃ composites with (a and c) $\Phi = 0.2$ and (b and d) $\Phi = 0.4$.

composite in dielectric performance. As shown in Fig. 6, the ρ_{DC} values of both the composites are comparable at room temperature when Φ is less than 0.4, whereas the ρ_{DC} of PEI/ α -Fe₂O₃ is much lower than that of PEI/BaTiO₃ at the higher Φ . This is because the interparticle distance becomes small enough for tunneling conduction to occur owing to high loading of particles. Fig. 8 shows the f dependences of the ϵ'_r and ϵ''_r of the two types of composites obtained at 40 °C and 160 °C. At 40 °C, although the ϵ'_r of PEI/ α -Fe₂O₃ is higher than that of PEI/BaTiO₃ in the lower f range, the ϵ''_r of PEI/ α -Fe₂O₃ is much larger than that of PEI/BaTiO₃. At 160 °C, however, ϵ'_r has comparable ϵ''_r values to PEI/BaTiO₃ except with $\Phi = 0.5$, and higher ϵ'_r than PEI/BaTiO₃. The dielectric characteristics at 1 kHz obtained at 160 °C are plotted as a function of Φ in Fig. 9. These results show that the PEI/ α -Fe₂O₃ composite was comparable to the PEI/BaTiO₃ composite in dielectric performance at 160 °C. The fitting curves for the ϵ'_r of the two types of composites are drawn in Fig. 9a in solid lines using Lichtenecker's logarithmic mixing rule. These theoretical curves well fit to the experimental results and give $\epsilon'_{r, BaTiO_3}$ of 86 and ϵ'_{r, Fe_2O_3} of 170, respectively. This value of 86 for BaTiO₃ is

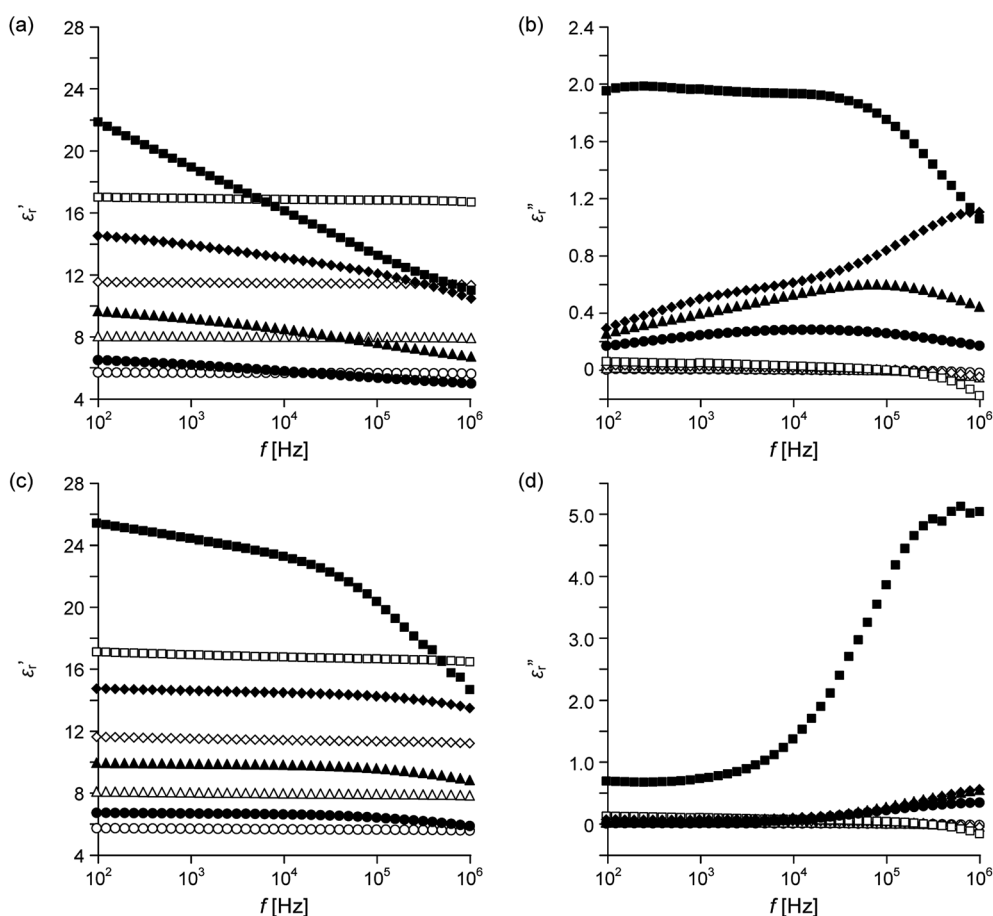


Fig. 8 Frequency f dependence of (a and c) ϵ'_r and (b and d) ϵ''_r of two types of composites with $\Phi = 0.2$ (circles), $\Phi = 0.3$ (triangles), $\Phi = 0.4$ (diamonds) and $\Phi = 0.5$ (squares) obtained at (a and b) 40 °C and (c and d) 160 °C. Open symbols, PEI/BaTiO₃; filled symbols, PEI/ α -Fe₂O₃.



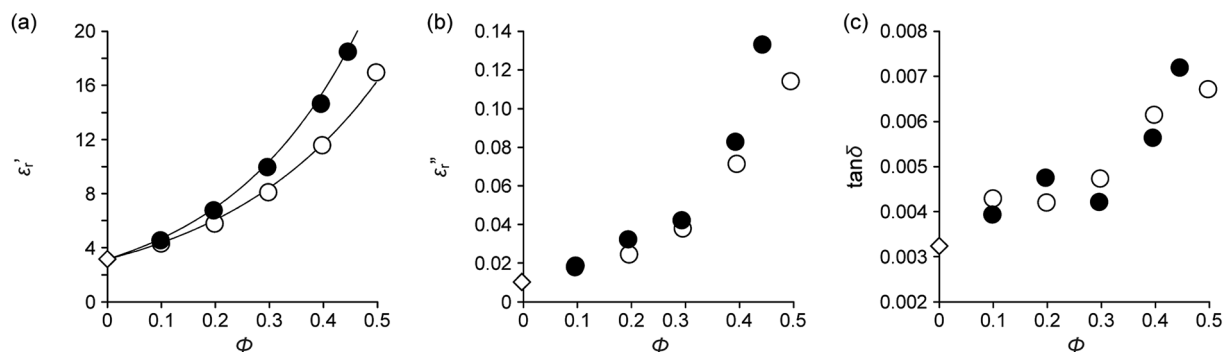


Fig. 9 (a) ϵ'_r , (b) ϵ''_r and (c) dissipation factor ($\tan \delta$) (1 kHz) of PEI (diamonds) and two types of composites (circles) obtained at 160 °C as a function of ϕ . Open symbols, PEI/BaTiO₃; filled symbols, PEI/ α -Fe₂O₃. (a) Solid lines show the fitting curves using Lichtenecker's logarithmic mixing rule.

consistent with some reported results; ϵ'_r BaTiO₃ is around 100.^{8,39}

Conclusion

The dielectric properties of polymer/ α -Fe₂O₃ composites strongly depended not only on the temperatures but also on the kind of polymer matrices. For engineering plastics such as PEI, PSF, PAR and PES, the ϵ'_r was highly enhanced at around 1 kHz by incorporation of α -Fe₂O₃ particles owing to Maxwell–Wagner polarization of free electrons in the α -Fe₂O₃ particles. This is probably because the π electrons in the aromatic structures of the engineering plastics strongly interact with the electrons in the α -Fe₂O₃ particles. Furthermore, the ϵ''_r for the engineering plastics became small at the elevated temperatures because the σ of the α -Fe₂O₃ particle was enhanced and therefore the relaxation frequency of Maxwell–Wagner polarization was shifted to higher f . PEI/ α -Fe₂O₃ composites exhibited highly improved dielectric properties at around 1 kHz, the high ϵ'_r and very low ϵ''_r at the elevated temperature above 120 °C. It was demonstrated that the PEI/ α -Fe₂O₃ composite was comparable to the PEI/BaTiO₃ composite in dielectric performance at 160 °C. Because the cost of α -Fe₂O₃ is much lower than that of BaTiO₃, the PEI/ α -Fe₂O₃ composites might be promising as a low-cost dielectric material for high-temperature applications.

Acknowledgements

SEM observation was carried out by Mr Yasuhiro Takatani at Toyota Central R&D Labs Inc. The authors appreciate his help.

References

- W. J. Sarjeant, J. Zirnheld, F. W. MacDougall, J. S. Bowers, N. Clark, I. W. Clelland, R. A. Price, M. Hudis, I. Kohlberg, G. McDuff, I. McNab, S. G. Parler Jr and J. Prymak, in *Handbook of low and high dielectric constant materials and their applications*, ed. H. S. Nalwa, Academic Press, London, 1999, vol. 2, ch. 9, pp. 423–491.
- Q. Wang and L. Zhu, *J. Polym. Sci., Part B: Polym. Phys.*, 2011, **49**, 1421–1429.
- Z. M. Dang, J. K. Yuan, J. W. Zha, T. Zhou, S. T. Li and G. H. Hu, *Prog. Mater. Sci.*, 2012, **57**, 660–723.
- S. D. Cho, S. Y. Lee, J. G. Hyun and K. W. Paik, *J. Mater. Sci.: Mater. Electron.*, 2005, **16**, 77–84.
- P. Kim, S. C. Jones, P. J. Hotchkiss, J. N. Haddock, B. Kippelen, S. R. Marder and J. W. Perry, *Adv. Mater.*, 2007, **19**, 1001–1005.
- J. Lu and C. P. Wong, *IEEE Trans. Dielectr. Electr. Insul.*, 2008, **15**, 1322–1328.
- K. W. Jang and K. W. Paik, *J. Appl. Polym. Sci.*, 2008, **110**, 798–807.
- P. Kim, N. M. Doss, J. P. Tillotson, P. J. Hotchkiss, M. J. Pan, S. R. Marder, J. Li, J. P. Calame and J. W. Perry, *ACS Nano*, 2009, **3**, 2581–2592.
- Y. Kobayashi, A. Kurosawa, D. Nagao and M. Konno, *Polym. Eng. Sci.*, 2009, **49**, 1069–1075.
- A. Choudhury, *Mater. Chem. Phys.*, 2010, **121**, 280–285.
- L. Xie, X. Huang, C. Wu and P. Jiang, *J. Mater. Chem.*, 2011, **21**, 5897–5906.
- S. Siddabattuni, T. P. Shuman and F. Dogan, *Mater. Sci. Eng., B*, 2011, **176**, 1422–1429.
- M.-F. Lin, V. K. Thakur, E. J. Tan and P. S. Lee, *RSC Adv.*, 2011, **1**, 576–578.
- Y. Song, Y. Shen, H. Liu, Y. Lin, M. Li and C. W. Nan, *J. Mater. Chem.*, 2012, **22**, 16491–16498.
- X. Wu, Z. Chen and Z. Cui, *Compos. Sci. Technol.*, 2013, **81**, 48–53.
- K. Hayashida and Y. Matsuoka, *Carbon*, 2012, **60**, 506–513.
- K. Hayashida, Y. Matsuoka and Y. Takatani, *RSC Adv.*, 2014, **4**, 33530–33536.
- C. Fettkenhauer, J. Glenneberg, W. Münchgesang, H. S. Leipner, G. Wagner, M. Diestelhorst, C. Pientischke, H. Beige and S. G. Ebbinghaus, *RSC Adv.*, 2014, **4**, 40321–40329.
- W. Lei, R. Wang, D. Yang, G. Hou, X. Zhou, H. Qiao, W. Wang, M. Tian and L. Zhang, *RSC Adv.*, 2015, **5**, 47429–47438.



- 20 W. Yang, S. Yu, S. Luo, R. Sun, W.-H. Liao and C.-P. Wong, *J. Alloys Compd.*, 2015, **620**, 315–323.
- 21 Y. Feng, W. L. Li, Y. F. Hou, Y. Yu, W. P. Cao, T. D. Zhang and W. D. Fei, *J. Mater. Chem. C*, 2015, **3**, 1250–1260.
- 22 R. B. Hilborn Jr, *J. Appl. Phys.*, 1965, **36**, 1553–1557.
- 23 K. Iwachi, S. Yamamoto, Y. Bando and N. Koizumi, *Bull. Inst. Chem. Res., Kyoto Univ.*, 1970, **48**, 159–169.
- 24 D. A. Sverjensky and N. Sahai, *Geochim. Cosmochim. Acta*, 1996, **60**, 3773–3797.
- 25 M. L. Jimenez, F. J. Arroyo, F. Carrique and U. Kaatz, *J. Phys. Chem. B*, 2003, **107**, 12192–12200.
- 26 J. A. Glasscock, P. R. F. Barnes, I. C. Plumb, A. Bendavid and P. J. Martin, *Thin Solid Films*, 2008, **516**, 1716–1724.
- 27 R. A. Lunt, A. J. Jackson and A. Walsh, *Chem. Phys. Lett.*, 2013, **586**, 67–69.
- 28 D. Dudić, M. Marinović-Cincović, J. M. Nedeljković and V. Djoković, *Polymer*, 2008, **49**, 4000–4008.
- 29 A. M. E. Sayed and W. M. Morsi, *J. Mater. Sci.*, 2014, **49**, 5378–5387.
- 30 D. Chen, H. Quan, Z. Huang, S. Luo, X. Luo, F. Deng, H. Jiang and G. Zeng, *Compos. Sci. Technol.*, 2014, **102**, 126–131.
- 31 C. Kittel, in *Introduction to Solid State Physics*, ed. C. Kittel, John Wiley & Sons, New York, 7th edn, 1996, ch. 8, pp. 197–232.
- 32 S. Mohanty and J. Ghose, *J. Phys. Chem. Solids*, 1992, **53**, 81–91.
- 33 A. Schönhals and F. Kremer, in *Broadband Dielectric Spectroscopy*, ed. F. Kremer and A. Schönhals, Springer-Verlag, Berlin, 2003, ch. 3, pp. 59–98.
- 34 D. Tan, L. Zhang, Q. Chen and P. Irwin, *J. Electron. Mater.*, 2014, **43**, 4569–4575.
- 35 Q. Li, L. Chen, M. R. Gadinski, S. Zhang, G. Zhang, H. Li, A. Haque, L. Q. Chen, T. Jackson and Q. Wang, *Nature*, 2015, **523**, 576–580.
- 36 M. N. Teerenstra, P. A. M. Steeman, W. Iwens, A. Vandervelden, D. R. Suwier, B. V. Mele and C. E. Koning, *e-Polym.*, 2003, **3**, 596–607.
- 37 H.-B. Tsai and Y.-D. Lee, *J. Polym. Sci., Part A: Polym. Chem.*, 1987, **25**, 1505–1515.
- 38 N. Erdman, R. Campbeli and S. Asahina, *Microsc. Today*, 2006, **14**, 22–25.
- 39 K. Hayashida, *RSC Adv.*, 2013, **3**, 221–227.
- 40 K. Hayashida and Y. Matsuoka, *Carbon*, 2015, **85**, 363–371.
- 41 G. E. Pike and C. H. Seager, *Phys. Rev. B: Solid State*, 1974, **10**, 1421–1434.
- 42 C. D. Lorenz and R. M. Ziff, *J. Chem. Phys.*, 2001, **114**, 3659–3661.
- 43 K. Hayashida and H. Tanaka, *Adv. Funct. Mater.*, 2012, **22**, 2338–2344.

